Cyclooxygenase-2 Inhibitor Induces Apoptosis in Breast Cancer Cells in an *In vivo* Model of Spontaneous Metastatic Breast Cancer

Gargi D. Basu,[1] Latha B. Pathangey,[1] Teresa L. Tinder,[1] Michelle LaGioia,[1] Sandra J. Gendler,[1,2] and Pinku Mukherjee[1]

[1]Mayo Clinic College of Medicine, Department of Biochemistry and Molecular Biology and [2]Tumor Biology Program, Scottsdale, Arizona

Abstract

Cyclooxygenase-2 (COX-2) inhibitors are rapidly emerging as a new generation of therapeutic drug in combination with chemotherapy or radiation therapy for the treatment of cancer. The mechanisms underlying its antitumor effects are not fully understood and more thorough preclinical trials are needed to determine if COX-2 inhibition represents a useful approach for prevention and/or treatment of breast cancer. The purpose of this study was to evaluate the growth inhibitory mechanism of a highly selective COX-2 inhibitor, celecoxib, in an *in vivo* oncogenic mouse model of spontaneous breast cancer that resembles human disease. The oncogenic mice carry the polyoma middle T antigen driven by the mouse mammary tumor virus promoter and develop primary adenocarcinomas of the breast. Results show that oral administration of celecoxib caused significant reduction in mammary tumor burden associated with increased tumor cell apoptosis and decreased proliferation *in vivo*. *In vivo* apoptosis correlated with significant decrease in activation of protein kinase B/Akt, a cell survival signaling kinase, with increased expression of the proapoptotic protein Bax and decreased expression of the antiapoptotic protein Bcl-2. In addition, celecoxib treatment reduced levels of proangiogenic factor (vascular endothelial growth factor), suggesting a role of celecoxib in suppression of angiogenesis in this model. Results from these preclinical studies will form the basis for assessing the feasibility of celecoxib therapy alone or in combination with conventional therapies for treatment and/or prevention of breast cancer. (Mol Cancer Res 2004;2(11):632–42)

Introduction

In the United States, breast cancer is the second most common cancer and contributes to 40,000 deaths in a year. If confined within the breast, the tumor can be surgically removed with an increased survival rate. However, primary tumors that metastasize to distant sites such as lymph nodes, lungs, liver, and brain correlate with poor prognosis. Complications from metastatic disease are the leading cause of cancer-related deaths. Mean survival for patients with metastatic breast cancer is 18 to 24 months. Response to chemotherapy or endocrine therapy in metastatic breast cancer patients is ~50% (1). Clearly, a need for development of novel therapies to enhance the existing triad of surgery, radiation, and chemotherapy is evident. Cyclooxygenase-2 (COX-2), the inducible form of the COX enzymes, catalyzes conversion of arachidonic acid to prostaglandin H_2, which is further converted to several other prostaglandins with diversified functions. Deregulation of COX-2 activity and downstream prostaglandins plays a vital role in carcinogenesis, inflammation, and tissue damage (2-5). COX-2 is overexpressed in many cancers including breast cancer, and the major functional prostaglandin in breast cancer is prostaglandin E_2 (PGE_2). Overexpression of COX-2 protein and PGE_2 during carcinogenesis is implicated in proliferation, invasion, apoptosis, immune suppression, and angiogenesis. COX-2 is induced by a variety of factors including tumor promoters, cytokines, growth factors, and hypoxia. Importantly, selective inhibition of this enzyme reduces adenocarcinoma formation and cancer progression in preclinical animal models (6-8). The first direct evidence of COX-2 function in cancers came from the study by Eberhart et al. (9), documenting significant elevations in COX-2 expression in 85% of human colorectal carcinomas and 50% of colorectal adenomas. COX-2 overexpression has since been found in many other human cancers including breast (10, 11), esophageal (12, 13), lung (14, 15), prostate (16, 17), bladder (18, 19), skin (20, 21), and pancreas (22, 23).

Studies with specific inhibitors of COX-2 enzyme have shown significant effects in reducing the incidence and progression of tumors in both animal models and in treatment of cancer patients (6-8). Studies to evaluate effects of COX-2-specific inhibitors in the treatment of breast cancer have started recently; therefore, data are limited. In animal studies, COX-2 inhibitors have shown promising results. In rat models of chemical carcinogenesis, COX-2 inhibitors significantly reduced incidence and size of mammary tumors (31, 32). COX-2 inhibitors were also effective in retarding tumor progression and metastasis in mouse models of injected breast cancer cell lines and in xenograft models of human breast cancer cells in nude mice (24, 33, 34). Clinically, COX-2 inhibitors have been

used in combination with other anticancer drugs or radiation therapy to treat solid tumors, mostly focusing on colon and colorectal cancers. Reports emerging from these studies strongly suggest that COX-2 inhibitors may emerge as a new generation of therapeutic drugs for cancer therapy. A recent report indicated that regular nonsteroidal anti-inflammatory drug use for 5 to 9 years was associated with a 21% reduction in the incidence of breast cancer and regular use for >10 years was associated with 28% reduction (35). This area of research is underexplored and more thorough preclinical trials are needed to further determine if COX-2 inhibition represents a useful approach to treatment of breast cancer.

Preclinical studies must precede clinical trials, and use of appropriate mouse models is key to the development of efficient therapeutic strategies. We have used in this study the oncogenic mice that carry the polyoma virus middle T antigen (MTag) driven by the mouse mammary tumor virus (MMTV) long terminal repeat promoter. These mice develop spontaneous tumors of the breast, which metastasize to the lungs and bone marrow. All mice are congenic on the C57BL/6 background to eliminate strain-specific modifier effects. In the MTag mice, mammary gland tumors are induced by the action of a potent tyrosine kinase activity associated with the polyoma virus MTag driven by the MMTV promoter (36). MTag specifically associates with and activates the tyrosine kinase activity of several c-*src* family members, eliciting tumors when a threshold level of gene product has been attained. In these mice, the MMTV promoter is transcriptionally active throughout all stages of mammary gland development, which results in widespread transformation of the mammary epithelium and the rapid production of multifocal mammary adenocarcinomas. Focal atypical lesions can be detected by whole mount as early as 21 days and palpable mammary gland tumors are detectable from ∼60 days onward. Tumor progression is quite rapid, reaching 10% of body weight by ∼20 to 24 weeks. All of the female mice get tumors. Tumors arise with synchronous kinetics and are highly fibrotic with dense connective tissue separating individual nests of tumor cells, a pathology that closely resembles scirrhous carcinomas of the human breast (37, 38). These mice exhibit metastasis in the lungs (60%) and micrometastasis in the bone marrow by 4 months of age (39). Therefore, the MTag mouse model is an appropriate model for human metastatic breast cancer in which to evaluate therapeutic strategies and to understand the mechanisms associated with therapy-induced growth inhibition. This is the first study to evaluate the efficacy and growth inhibitory mechanisms of celecoxib in an *in vivo* model of spontaneous metastatic breast cancer.

Results

Celecoxib Treatment Caused Significant Reduction in Primary Mammary Tumor Burden

Ten-week-old tumor-bearing female MTag mice were gavaged daily for 4 weeks with celecoxib at 5, 10, or 20 mg/ kg body weight. In mice, at 10 and 20 mg/kg dose, the concentration of celecoxib in the plasma ranges from 6.5 to 13 μmol/L at 2 hours and from 4.2 to 8 μmol/L at 4 hours post-celecoxib treatment (40). This dose is attainable clinically and

sufficient to inhibit PGE_2 (41). At 10 weeks, mice have small palpable tumors (1-2 tumors, ∼0.1-0.5 mg tumor weight). One hundred percent of the MTag mice have hyperplastic mammary glands by 6 to 8 weeks (starting at time of puberty). Because the MTag is a strong oncogene, driven by the MMTV promoter, 100% of the MTag mice develop multifocal tumors with palpable tumors in at least 1 to 2 glands (of 10 mammary glands in mice) by 10 weeks. Every gland is hyperplastic by this time and every gland has palpable tumors by 14 weeks. Complete blood count analysis including hemoglobin levels was done to determine cytopenia and/or anemia post-celecoxib treatment. Regardless of the celecoxib dose, there was no detectable change in their complete blood count or hemoglobin levels (data not shown) as compared with untreated MTag mice. Flow cytometric analysis of T cells, B cells, and natural killer cells revealed no change in treated versus control MTag mice, nor were there any signs of weight loss in treated mice (data not shown). This suggested that celecoxib was well tolerated in these mice with no detectable signs of toxicity. Mice were sacrificed at 14 weeks of age, tumors were removed, and serum was collected. Tumor burden in MTag mice treated with 10 and 20 mg/kg dose was significantly reduced ($P < 0.003$ for 10 mg/ kg and $P < 0.01$ for 20 mg/kg; Fig. 1). Note that in this study we started the treatment at 10 weeks when the mice had established tumors. The purpose of this study was to focus on the short-term effect of celecoxib on breast cancer cells *in vivo* at early times during tumor development and evaluate the mechanism of action of the drug on primary breast cancer cells. All mice were terminated at 14 weeks of age. The cumulative palpable tumors from 10 mammary glands at 14 weeks of age for individual mouse are presented in Fig. 1. Because metastasis in the MTag mice only develop between 19 and 24 weeks of age, we evaluated 6 MTag mice that received 20 mg/kg celecoxib and 10 vehicle-treated MTag mice between 20 and 24
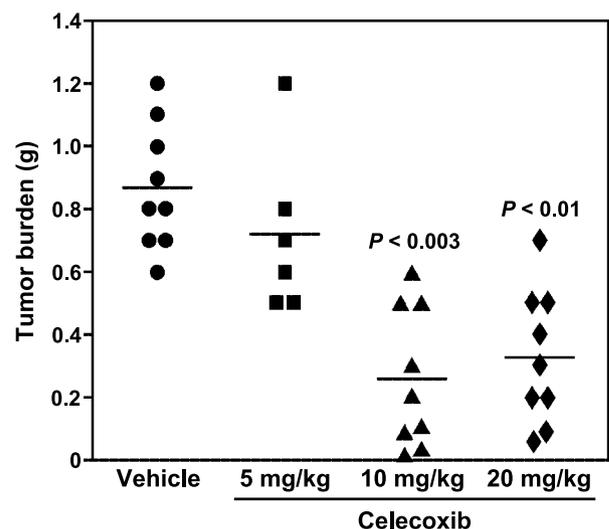

FIGURE 1. Reduced tumor burden in 14-week-old MTag mice post-celecoxib treatment. MTag mice were palpated weekly for presence of mammary tumors. Tumor weights plotted represent total tumor burden (including all mammary glands) per mice at 14 weeks of age (*n* = 9 mice for vehicle and 10 and 20 mg/kg celecoxib and *n* = 6 mice for 5 mg/kg celecoxib).

weeks of age. Gross microscopic examination of lungs revealed that the celecoxib-treated mice did not develop metastasis (0 of 6), whereas 6 of the 10 control mice developed lung metastasis (data not shown). These results are preliminary and we need to enroll more mice to the study to achieve statistical significance.

Celecoxib Induces Apoptosis in Breast Cancer Cells In vivo

We have reported recently that celecoxib induces growth inhibition of human and mouse breast cancer cells *in vitro* by simultaneously activating tumor cell apoptosis and inhibiting proliferation (42). Apoptosis of primary MTag tumor cells was determined by Annexin V/propidium iodide staining and flow cytometry. Data revealed significant increase in apoptotic cell population at 10 and 20 mg/kg celecoxib dose as compared with control MTag mice (39% in control mice versus 65% in 10 mg/kg dose, $P < 0.05$; 59% in 20 mg/kg dose, $P < 0.05$). The lowest dose (5 mg/kg) did not have a significant effect (Fig. 2A). Tumor cells from untreated MTag mice gave similar percentage of apoptotic cells ($\sim$ 35-40%) as vehicle-treated mice (data not shown). The high baseline apoptosis level in vehicle-treated and untreated mice is likely due to the method of isolating single cells. However, the 1.5- to 1.7-fold increase following celecoxib treatment was reproducibly observed.

We also evaluated celecoxib-induced apoptosis *in situ* by detection of DNA fragmentation using the terminal deoxynucleotidyl transferase–mediated dUTP nick end labeling (TUNEL) assay (43). We observed an increase in TUNEL-positive cells in celecoxib-treated tumor sections *in situ* as compared with control tumor sections, confirming the flow cytometry data (Fig. 2B). Representative immunohistochemical images of vehicle-treated and celecoxib-treated MTag tumor sections are shown at 100× magnification, demonstrating considerable TUNEL positivity in celecoxib-treated versus control MTag tumor sections.

Increased Bax and Decreased Bcl-2 in Tumor Lysate Derived from Celecoxib-Treated MTag Mice

The downstream signaling pathways involved in COX-2-induced apoptosis are not well understood, but at least three pathways have been suggested: Bcl-2-mediated pathway, nitric oxide pathway, and production of ceramide (44). Because it has been shown previously in cell lines that celecoxib-induced apoptosis is associated with decreased Bcl-2 (an antiapoptotic protein) and increased Bax (a proapoptotic protein), we evaluated the levels of Bcl-2 and Bax by Western blot analysis of whole MTag tumor lysate post-celecoxib treatment. Treatment with celecoxib at 10 and 20 mg/kg induced increased expression of Bax (inducer of apoptosis) in all five mice tested as compared with vehicle-treated tumors (Fig. 3A). The increase was most pronounced at the 10 mg/kg dose of celecoxib. Simultaneously, there was decrease in Bcl-2 (inhibitor of apoptosis) protein expression in the 10 and 20 mg/kg dose of celecoxib (Fig. 3B). Untreated MTag tumor lysate was used as positive control in the first lane. These tumor lysates were prepared from 21-week-old MTag tumors, whereas the treated mice were at 14 weeks of age. This could explain the difference in protein expression observed
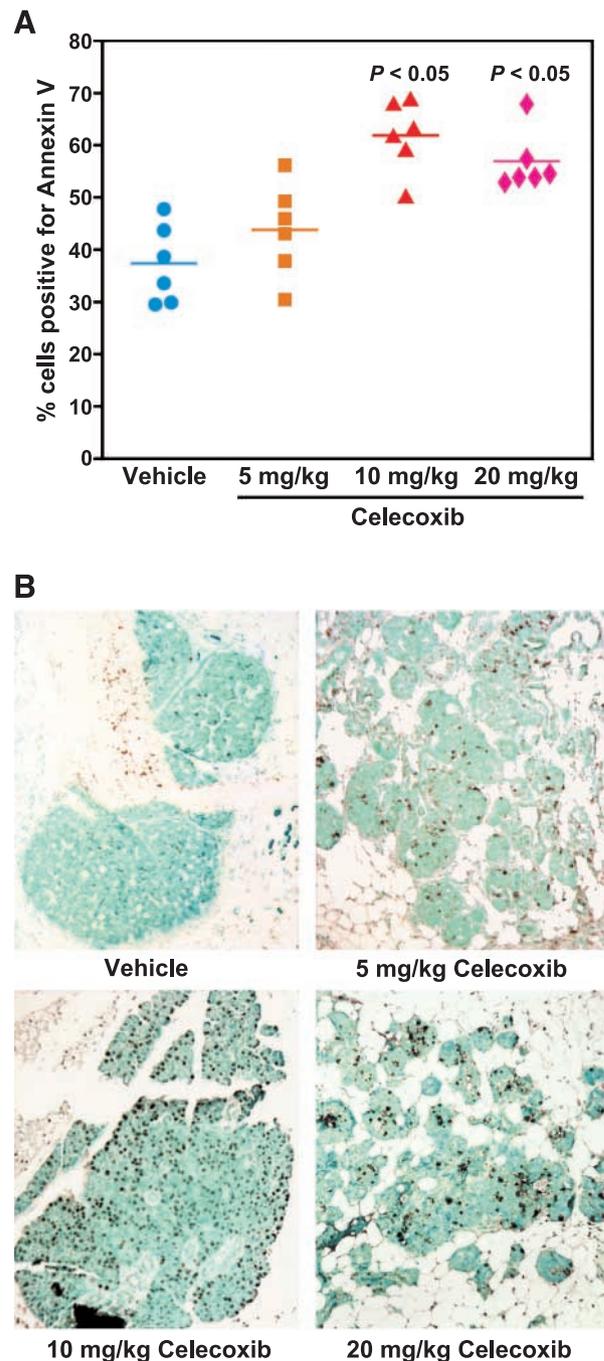
FIGURE 2. A. Increase in Annexin V–positive cells in celecoxib-treated MTag tumors *in vivo*. Tumor cells derived from vehicle-treated or celecoxib (5, 10, or 20 mg/kg body weight)–treated MTag mice were stained with Annexin V conjugated with FITC and propidium iodide, and percentage apoptotic cells (cells positive for Annexin V) were analyzed by flow cytometry. $n = 6$ mice per treatment group. *P*, significant difference between celecoxib-treated groups and vehicle control. **B.** Increase in TUNEL-positive cells in celecoxib-treated MTag tumors *in situ*. Light microscopic image of TUNEL-positive cells visualizing apoptosis *in situ* from mammary gland tumor sections isolated from vehicle and 5, 10, and 20 mg/kg celecoxib-treated MTag mice. *Brown,* apoptotic cells. All images are representative of five standardized fields from six separate mice. Magnification, ×100.
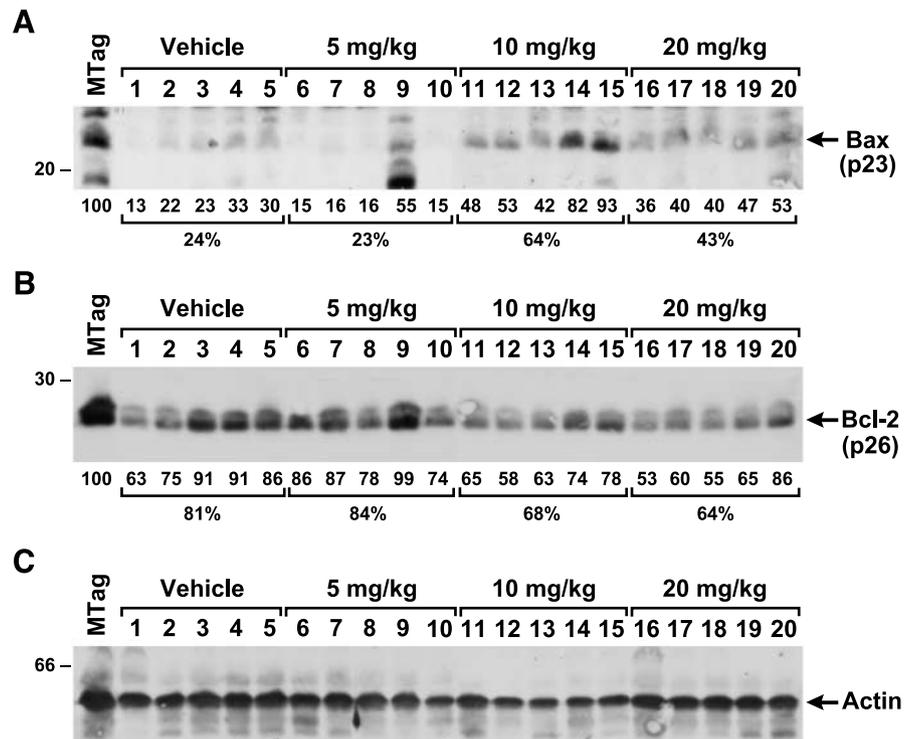
FIGURE 3. Increase in the proapoptotic protein Bax and decrease in the antiapoptotic protein Bcl-2 post-celecoxib treatment. Western blot analysis of Bax and Bcl-2 protein levels in mammary gland tumor lysates from vehicle and celecoxib (5, 10, and 20 mg/kg)–treated MTag mice; 100 μg of protein were loaded per lane. $n = 5$ individual mice. *Numbers below each lane,* percentage of protein expression compared with MTag lysate, which was set to equivalent of 100% as determined by densitometric analysis. Average percentage expression for each treatment group ($n = 5$ mice). *P,* significant difference between treatment groups and vehicle control. β-Actin is used as the protein loading control for all tumor lysates.

between vehicle-treated and untreated MTag tumors. Tumor lysate from 14-week-old MTag mice have similar Bcl-2 and Bax levels as vehicle-treated tumors (data not shown). Densitometric analysis of the Western blots indicates significant increase in Bax protein levels between vehicle-treated and 10 mg/kg ($P < 0.05$) and 20 mg/kg ($P < 0.06$) celecoxib-treated tumor lysates. Similarly, significant decrease in Bcl-2 was observed between vehicle-treated and 5 mg/kg celecoxib–treated mice versus 10 mg/kg ($P < 0.05$) and 20 mg/kg ($P < 0.05$) celecoxib-treated groups. All comparisons are between 14-week-old vehicle-treated tumors and age-matched celecoxib-treated tumors. Thus, data suggest that celecoxib-induced apoptosis in MTag tumor cells *in vivo* is associated with an elevated expression of Bax and reduced expression of Bcl-2 proteins. These results give further credence to the flow cytometry and TUNEL data, confirming that celecoxib induces apoptosis *in vivo* in a highly aggressive and metastatic breast cancer model.

Reduced Phosphorylation of Akt in Tumor Lysate Derived from Celecoxib-Treated MTag Mice

Protein kinase B/Akt is a serine/threonine protein kinase that is involved in promoting cell survival signals through the phosphatidylinositol 3-kinase (PI3K) pathway leading to inactivation of a series of proapoptotic proteins. These kinase activities are frequently deregulated in human disease including cancer (45). Akt represents a key signaling component in cell survival by activating downstream proapoptotic proteins and caspases (46-48). Celecoxib has been shown recently to induce apoptosis of cancer cells by blocking Akt activation in cultured prostate cancer cells (49, 50). To explore whether inhibition of

Akt activation may be linked to the observed *in vivo* apoptosis in MTag tumors, we determined the effect of *in vivo* celecoxib administration on phosphorylation of Akt (at Ser[473] in the carboxyl terminus) in MTag tumors. Data show that celecoxib substantially suppresses phosphorylation of Akt in MTag tumors. Two of five mice in the 5 mg/kg dose showed reduced phosphorylation, whereas four of five in 10 mg/kg and five of five mice in 20 mg/kg dose showed reduced Akt activation (Fig. 4). Densitometric analysis clearly indicates significant down-regulation of Akt phosphorylation in celecoxib-treated tumors as compared with vehicle-treated tumors ($P < 0.05$ for 10 and 20 mg/kg celecoxib). All tumors showed approximately equivalent levels of the Akt protein as shown in Fig. 4 (*bottom*). This result clearly suggested the involvement of the Akt pathway in induction of apoptosis *in vivo* in our mouse model of spontaneous breast cancer. Akt represents a key signaling component in cell survival by activating downstream proapoptotic proteins and caspases (46-48). Because we observed a decrease in Akt phosphorylation and increase in proapoptotic protein (Bax), we determined if caspases were activated post-celecoxib treatment. MTag tumor cells treated with celecoxib *in vitro* (20, 40, and 60 μmol/L) were analyzed for activation of effector caspase-3 and caspase-7. Most apoptotic signals induce intracellular cleavage of caspase-3 and caspase-7 and convert them into active forms. Caspase activity is presented as fluorescence emission, which is directly proportional to caspase-3/7 activities. Increase in fluorescence emission was observed with increasing dose of celecoxib, which correlates with increase in active forms of caspase-3 and caspase-7. Table 1 illustrates the fluorescence emission for untreated versus
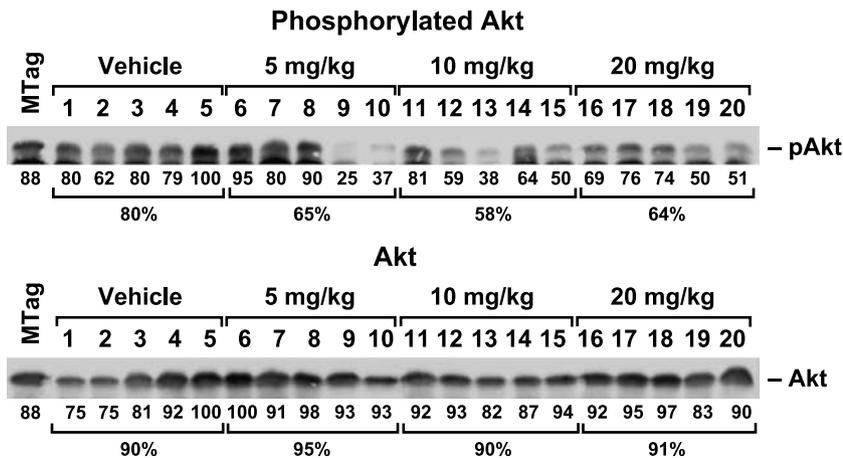
Phosphorylated Akt

MTag	Vehicle					5 mg/kg					10 mg/kg					20 mg/kg				
	1	2	3	4	5	6	7	8	9	10	11	12	13	14	15	16	17	18	19	20

— pAkt

88	80	62	80	79	100	95	80	90	25	37	81	59	38	64	50	69	76	74	50	51
			80%					65%					58%					64%		

Akt

MTag	Vehicle					5 mg/kg					10 mg/kg					20 mg/kg				
	1	2	3	4	5	6	7	8	9	10	11	12	13	14	15	16	17	18	19	20

— Akt

88	75	75	81	92	100	100	91	98	93	93	92	93	82	87	94	92	95	97	83	90
			90%					95%					90%					91%		

FIGURE 4. Decreased phosphorylation of protein kinase B/Akt post-celecoxib treatment. Western blot analysis of phospho-Akt (*pAkt*) and Akt protein levels in mammary gland tumor lysates from vehicle and celecoxib (5, 10, and 20 mg/kg)–treated MTag mice; 100 μg of protein were loaded per lane. $n = 5$ individual mice. *Numbers below each lane,* percentage of protein expression compared with mouse expressing the most protein, which was set equivalent to 100% as determined by densitometric analysis. Average percentage expression for each treatment group ($n = 5$ mice). *P,* significant difference between treatment groups and vehicle control.

celecoxib-treated MTag tumor cells. Significant increase in fluorescence emission was observed in 40 and 60 μmol/L celecoxib-treated cells compared with untreated or vehicle-treated cells ($P < 0.05$ and 0.01, respectively).

Celecoxib Inhibits Tumor Cell Proliferation

Antiproliferative effect of *in vivo* celecoxib treatment was determined by *in situ* immunohistochemical analysis of MTag tumor sections stained with proliferating cell nuclear antigen (PCNA). A representative light microscope image suggests inhibition of proliferation in MTag tumors *in vivo* with 10 and 20 mg/kg celecoxib treatment (Fig. 5). PCNA protein levels peak during the S phase of the cell cycle and is almost undetectable in other phases of the cycle. Vehicle and 5 mg/kg celecoxib treatments show almost every cell expressing PCNA, indicative of highly proliferative cells (Fig. 5A and B). With 10 and 20 mg/kg treatment, fewer cells expressed PCNA staining, suggestive of fewer cells undergoing proliferation (Fig. 5C and D). A lymph node within an untreated mammary tumor section shows only a few proliferating cells, confirming the specificity of the stain (Fig. 5E). Staining specificity is further confirmed with second antibody control (Fig. 5F).

Celecoxib Treatment Significantly Reduced Serum Levels of PGE₂ In vivo

Next, we analyzed sera and tumor lysate from celecoxib-treated and vehicle-treated MTag mice for PGE₂ levels to assess

Table 1. Caspase-3 and Caspase-7 Activity of MTag Cells Treated with Celecoxib

Treatment	Caspase-3/7 Activity (Fluorescence Emission)
Vehicle	$1 \times 10^6 \pm 2.0 \times 10^5$
Celecoxib (20 μmol/L)	$2 \times 10^6 \pm 1.6 \times 10^5$
Celecoxib (40 μmol/L)	$4 \times 10^6 \pm 2.2 \times 10^5$*
Celecoxib (60 μmol/L)	$5 \times 10^6 \pm 2.0 \times 10^5$*

NOTE: Spectrofluorometric analysis of lysates prepared from 48-hour vehicle-treated and celecoxib (20, 40, and 60 μmol/L)–treated MTag cells. Activity of caspase-3 and caspase-7 was monitored by enzymatic cleavage using a fluorescence microplate reader with excitation at 485 ± 10 nm and emission detection at 530 ± 12.5 nm. Mean ± SD of three experiments.
*$P < 0.01$, significant difference between vehicle control and celecoxib treatment.

COX-2 activity *in vivo*. COX-2 converts arachidonic acid to bioactive prostaglandins. It has been shown that COX-2-derived PGE₂ is the major prostaglandin produced by breast cancer cells and may be required for the angiogenic switch leading to initiation and progression of mammary cancer in a MMTV-COX-2 transgenic mouse model (51). Production of secreted PGE₂ is an appropriate measure of COX-2 activity in the MTag mouse model. PGE₂ is unstable *in vivo* and
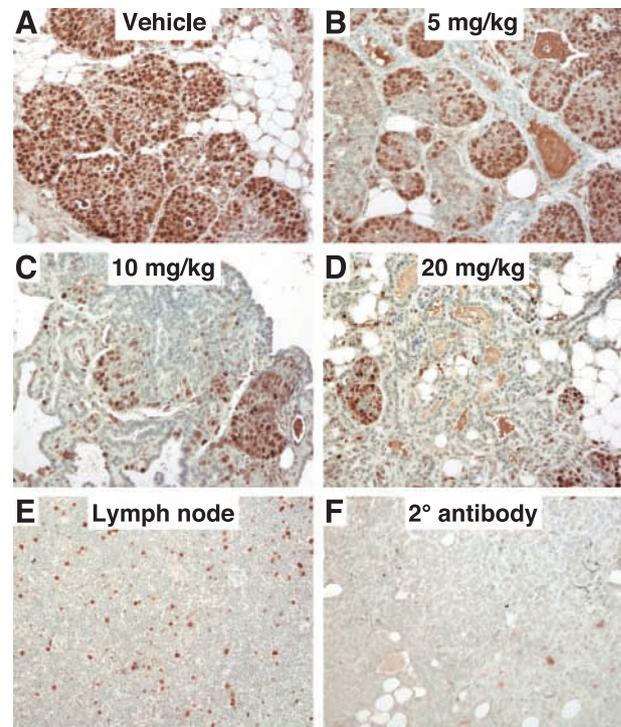

FIGURE 5. Celecoxib-induced inhibition of tumor cell proliferation *in vivo* in a dose-dependent manner. Light microscopy images of PCNA staining of mammary tumor sections from vehicle-treated (**A**) and celecoxib (5, 10, and 20 mg/kg)–treated (**B-D**) MTag mice. All images are representative of five standardized fields from six separate experiments. Inhibition of proliferation is most evident at 10 and 20 mg/kg dose of celecoxib. Lymph node section (**E**) and second antibody staining (**F**) are shown as controls. Magnification, ×200.

measurement of the metabolites is necessary to provide a reliable estimate of actual PGE_2 production. Thus, we measured PGE_2 metabolite (PGEM; i.e., 13,14-dihydro-15-keto prostaglandin A_2) using a commercially available ELISA. A significant reduction in serum PGEM is observed in 10 and 20 mg/kg celecoxib-treated MTag mice as compared with pretreatment and vehicle-treated mice (2,000 pg/mL in vehicle-treated mice versus <1,000 pg/mL in 10 mg/kg celecoxib-treated mice, $P < 0.01$; Fig. 6A). Similar reduction in PGEM was observed in tumor lysates (data not shown). Note that the serum PGEM levels never reached the values observed in nontumor C57BL/6 mice of 300 pg/mL (Fig. 6A). This suggests that, although celecoxib was partially effective in reducing PGEM levels, treatment was not sufficient to completely reverse the up-regulation of PGE_2 levels in MTag mice because these mice were not completely tumor free.

To test if celecoxib had a direct effect on COX-2 protein expression in the tumor, we evaluated COX-2 protein expression in tumor lysates from vehicle-treated and celecoxib-treated MTag tumors. MTag tumors from untreated and vehicle-treated mice expressed higher levels of COX-2 (Fig. 6B) as compared with celecoxib-treated (10 and 20 mg/kg) tumors, indicating that celecoxib has a direct effect on COX-2 protein expression

in vivo. Densitometric analysis showed some difference between vehicle-treated and 10 or 20 mg/kg celecoxib-treated tumors ($P < 0.07$). However, the direct effect of celecoxib on COX-2 protein expression was less significant ($P < 0.07$) than its effect on COX-2 activity as measured by PGE_2 levels.

Celecoxib Treatment Reduced Vascular Endothelial Growth Factor Levels In vivo

It has been shown recently that COX-2-induced PGE_2 stimulated the expression of angiogenic regulatory genes including vascular endothelial growth factor (VEGF) in mammary tumor cells isolated from COX-2 transgenic mice and that treatment with indomethacin (nonspecific COX inhibitor) suppressed the expression of these genes *in vitro* (51). We therefore evaluated levels of *in vivo* VEGF protein levels in the tumor microenvironment of MTag tumors postcelecoxib treatment. Treatment with celecoxib (10 or 20 mg/kg) reduced VEGF levels in the tumor lysate in four of six treated mice as compared with vehicle-treated MTag tumors ($P < 0.05$; Fig. 7). No reduction was observed in mice treated with 5 mg/kg celecoxib. Untreated MTag tumor lysate had similar levels as vehicle-treated MTag mice (data not shown). Similar reduction in circulating VEGF levels was also

FIGURE 6. A. Dose-dependent inhibition of PGE_2 synthesis in serum of celecoxib-treated MTag mice. PGEM levels in serum were determined using specific ELISA (pg/mL serum). Serum from mice was collected either before treatment commenced or after 4 weeks of celecoxib treatment. *P,* significant difference between celecoxib-treated and untreated (pretreatment) or vehicle-treated mice. PGE_2 levels are also compared with serum from age-matched non-tumor-bearing wild-type C57BL/6 mice. Significant inhibition is evident at 10 and 20 mg/kg dose. **B.** Decrease in COX-2 protein expression is not significant in MTag tumors post-celecoxib treatment ($n = 5$ mice). Western blot analysis of tumor lysates from untreated, vehicle-treated, and celecoxib (5, 10, and 20 mg/kg)−treated MTag mice; 100 μg of protein were loaded per lane. All tumor lysates expressed COX-2. Untreated and vehicle-treated tumors expressed higher levels of COX-2 than tumor lysates from celecoxib (10 and 20 mg/kg)−treated mice. *Numbers below each lane,* percentage of protein expression compared with mouse expressing the most protein, which was set equivalent to 100% as determined by densitometric analysis. Average percentage expression for each treatment group ($n = 5$ mice). β-Actin is used as the protein loading control for all tumor lysates.
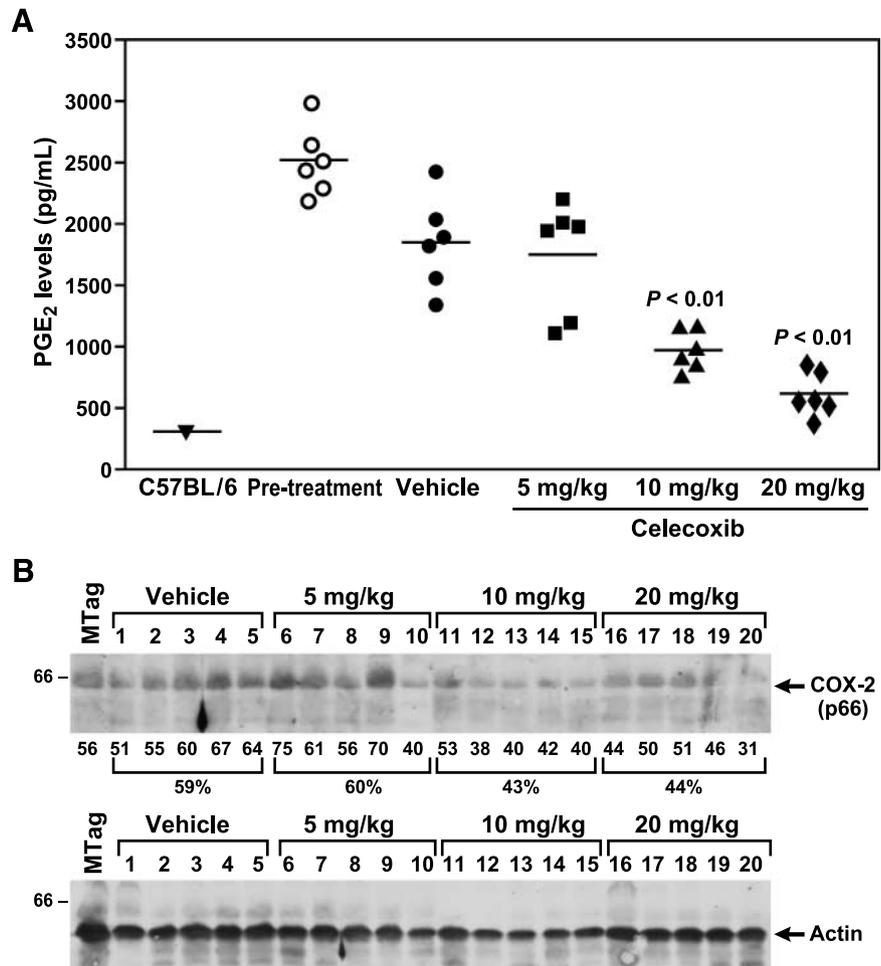
observed. Serum levels of VEGF in untreated or vehicle-treated 14-week-old MTag mice were found to be between 150 and 400 pg/mL, whereas in the mice treated with celecoxib (10 or 20 mg/kg) the levels ranged from 20 to 90 pg/mL. In some of the treated mice, the VEGF levels were too low to be detected by ELISA. Preliminary histologic evaluation also suggests the presence of fewer blood vessels in the celecoxib-treated tumor sections versus control tumor using the Masson's trichrome staining. A representative picture of vehicle, 5, 10, and 20 mg/kg celecoxib-treated MTag tumor is shown in Fig. 7B.

Discussion

We show for the first time that *in vivo* treatment with celecoxib causes significant reduction in mammary gland tumor burden in a mouse model of spontaneous breast cancer. Recently, we have evaluated 6 MTag mice that received 20 mg/kg celecoxib and 10 control MTag mice between 20 and 24 weeks of age. None of the celecoxib-treated mice developed lung metastasis, whereas 5 of the 10 control mice developed lung metastasis (data not shown).

Tumor reduction was associated with induction of tumor cell apoptosis *in vivo*. Investigation into the potential molecular pathway revealed that treatment with celecoxib caused reduction in activation of antiapoptotic/prosurvival kinase (Akt). Increased apoptosis was associated with increased expression of the proapoptotic protein Bax and decreased expression of the antiapoptotic protein Bcl-2. Concurrently, we observed decreased tumor cell proliferation and decreased synthesis of VEGF in mammary gland tumors treated with celecoxib *in vivo*, most probably associated with decreased PGE_2 synthesis.

The importance of this study lies in the use of a mouse model system that resembles human disease in many aspects of tumor progression. The MTag tumors start as hyperplasia, like early proliferative lesions seen in the human breast; show indication of histologic progression to malignant mammary adenocarcinomas and metastasis; are heterogenous with respect their malignant potential; and trigger signaling pathways inactive in normal breast epithelium (38). One of the pathways that is activated in these mice is the arachidonic acid/COX-2 pathway (52), similar to that described in many human breast cancers. Furthermore, we have shown recently that COX-2 protein and its downstream product PGE_2 were highly elevated in human breast tumors and lymph node metastasis compared with normal tissue, with the highest expression being observed in lymph node metastasis (53). There was a direct correlation between increased COX-2 and PGE_2 expression with impaired immune cell function in newly diagnosed stage I and II breast cancer patients (53). Our observations are similar to the reports that have shown significant elevation of COX-2 protein levels in 43% of human invasive breast cancers and 63% of ductal carcinomas *in situ* (11, 54). Thus, the MTag model offers the potential to evaluate chemoprevention with a highly specific COX-2 inhibitor, celecoxib.

Celecoxib has been shown to target multiple pathways of tumorigenesis including proliferation, apoptosis, angiogenesis, invasion, and tumor-induced immune suppression in various
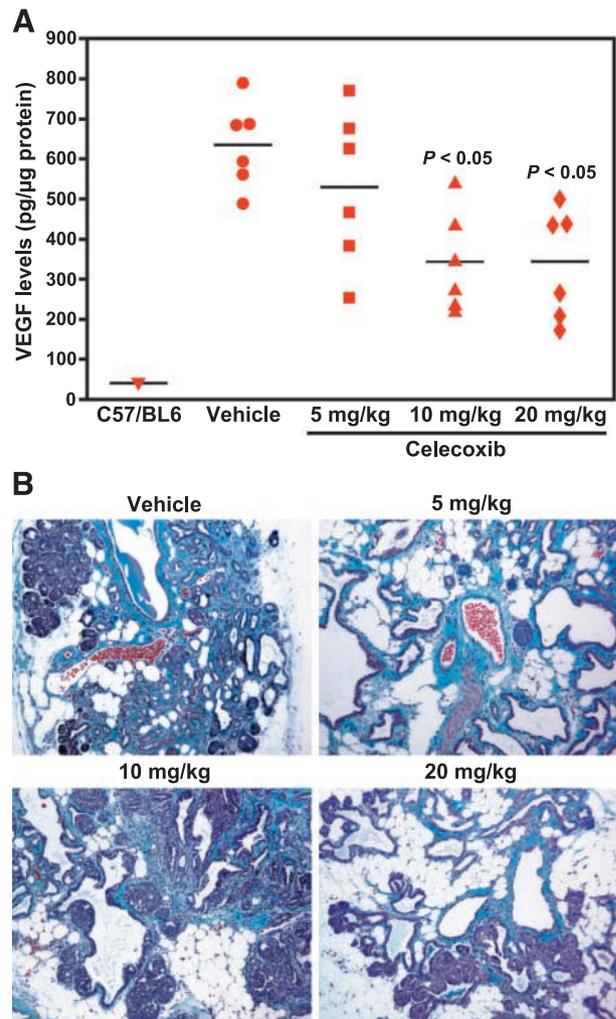

FIGURE 7. A. Decreased VEGF levels in MTag tumors from celecoxib-treated mice. VEGF levels were determined in the tumor lysates using specific ELISA (pg/μg protein lysate). Tumor lysate was prepared from untreated, vehicle-treated, and celecoxib (5, 10, and 20 mg/kg)–treated MTag mice. *P*, significant difference between celecoxib-treated and vehicle-treated mice. Values are also compared with mammary gland lysate from age-matched non-tumor-bearing wild-type C57BL/6 mice. Significant inhibition is evident at 10 and 20 mg/kg dose. **B.** Fewer blood vessels in 10 and 20 mg/kg celecoxib-treated tumor sections compared with vehicle-treated tumor. Blood vessels in MTag tumor sections were histologically evaluated by Masson's trichrome. This method stains fibrous tissue and stroma green. Blood vessels containing RBC stain bright red. Fewer blood vessels in the tumor section of the celecoxib-treated tumors (10 and 20 mg/kg) relative to those obtained from vehicle-treated animals. Magnification, ×100.

breast tumor cell lines. The current report by Chang et al. (51) supports the concept that COX-2 may provide an early target for breast cancer prevention. We show that early intervention with celecoxib causes reduced primary tumor burden in the MTag model (Fig. 1). We further show that reduced PGE_2 synthesis (Fig. 6A) and reduced PI3K/Akt kinase activation (Fig. 4) post-celecoxib treatment may be the mechanism(s) underlying enhanced tumor cell apoptosis (Fig. 2) and reduced tumor cell proliferation (Fig. 5) *in vivo*. Our data are in line with the recent *in vitro* study in prostate cancer cell lines, where

it was shown that celecoxib induces apoptosis by blocking or suppressing Akt activation (50). The PI3K/Akt pathway is typically activated in response to oncogenes that bind to receptor kinases at the plasma membrane and lead to the activation of PI3K (55, 56). Activated Akt targets multiple factors involved in cell proliferation, migration, and survival/apoptosis. Mechanistically, activated Akt is known to trigger several cyclins including cyclin D1 that affects all stages of the cell cycle and induces downstream proliferation (56). Preliminary data suggest decreased levels of cyclin D1 in tumor lysates of mice treated with celecoxib, with significant arrest of the mammary tumor cells at the G_2-M checkpoint phase of cell cycle (data not shown). Thus far, our results implicate the PI3K/Akt pathway to be critical in the celecoxib-induced apoptosis and inhibition of tumor cell proliferation. However, other pathways such as the Raf/mitogen-activated protein kinase–extracellular signal-regulated kinase/mitogen-activated protein kinase pathway may also be affected by celecoxib, and future studies will be designed to evaluate these pathways *in vivo* in the MTag mouse model. One potential mechanism that has been associated with PGE_2-related inhibition of apoptosis is that PGE_2 reduces the basal apoptotic rate by increasing the level of antiapoptotic proteins such as Bcl-2 (54, 57). Our *in vivo* data support this concept, because inhibiting PGE_2 production by targeting COX-2 activity in the MTag tumors led to decrease in Bcl-2 protein levels and concurrent increase in the proapoptotic protein Bax (Fig. 3A and B) as well as activate effector caspase-3 and caspase-7 (Table 1).

Finally, angiogenesis plays a crucial role in tumor development and progression. COX-2-dependent PGE_2 is a potent inducer of angiogenesis *in vivo* and induces expression of angiogenic regulatory proteins such as VEGF (51, 58, 59). It has been shown recently that overexpression of COX-2 in the mammary gland by MMTV promoter induces mammary carcinogenesis and that the major prostaglandin that is produced in these tumors is PGE_2 (51, 54). These authors further defined the role of COX-2-dependent PGE_2 production in transforming local tumors to invasive cancer by triggering a so-called angiogenic switch by increasing expression of proangiogenic mediators such as VEGF and its receptors. Thus, we examined whether celecoxib treatment *in vivo* was effective in reducing the exaggerated VEGF levels observed in MTag tumors and in the serum. Significant decrease in levels of VEGF in the mammary gland tumors accompanied by fewer blood vessels in the celecoxib-treated tumor sections versus control was observed (Fig. 7), once again suggesting a role of COX-2 and PGE_2 in mediating angiogenesis in the polyoma virus MTag-induced breast tumors. Although additional mechanisms are involved in mediating the angiogenic effects of COX-2, our data suggest that COX-2 influences angiogenesis at least in part by enhancing VEGF secretion by tumor endothelial cells. Additional studies are needed to fully elucidate the complex events involved in COX-2-mediated angiogenesis in our model. Our data clearly show extensive down-regulation of PGE_2 in serum (Fig. 6A) post-celecoxib treatment *in vivo*. PGE_2 binds to cell surface receptors that belong to the family of seven-transmembrane domain G protein-coupled receptors, designated EP1, EP2, EP3, and EP4 (54, 60). Future studies will determine the pattern of prostanoid receptor distribution in the MMTV-MTag mice and whether COX-2 inhibitors can modulate prostanoid receptor expression and its activation state. Although we suggest that PGE_2 down-regulation may be in part responsible for the reduced VEGF levels, we fully recognize that much work is required to define a direct relationship between PGE_2 and VEGF and that other pathways and angiogenic markers may be involved. We also acknowledge that the effect of celecoxib in the MTag mice may be COX independent; indeed, we do not see a dramatic down-regulation of COX-2 expression in celecoxib-treated compared with vehicle-treated mice (Fig. 6B). However, we must point out that we have published that the MTag tumors overexpress COX-2 and the expression increases as tumors progress and that the PGE_2 levels are significantly decreased with celecoxib treatment.

In summary, celecoxib treatment may exert its antiproliferative, antiangiogenic, and proapoptotic effects by regulating the PGE_2-prostanoid receptor–associated pathways and by decreasing PI3K/Akt phosphorylation. This leads to significant reduction in primary breast tumor burden. Furthermore, this effect may or may not be dependent on down-regulation of COX-2 protein expression in the tumor. Thus, we believe that COX-2 inhibitors not only represents a future therapeutic option for the treatment of human breast cancer in combination with standard therapies but also may be considered as a potent chemopreventive agent for individuals with high risk of developing breast cancer and for individuals with high risk of disease relapse.

Materials and Methods

Generation of MTag Mouse Model

MTag oncogenic mice was originally a kind gift from Dr. W.J. Muller (McGill University, Toronto, Ontario, Canada; ref. 36). MTag male mice were mated to C57BL/6 mice to maintain the MTag mice as heterozygous. Approximately 50% of the pups carry the oncogene, and in these pups, ∼ 50% are females that develop mammary gland adenocarcinomas and are used for the experiments. PCR was used to routinely identify the MTag oncogene. PCR was carried out as described previously (39). Primer pairs for MTag transgene are 5′-AGTCACTGCT-ACTGCACCCAG-3′ (282-302 bp) and 5′-CTCTCCTCAGT-TCCTCGCTCC-3′ (817-837 bp). The amplification program for MTag consisted of 1 cycle of 5 minutes at 95°C and 40 cycles of 30 seconds at 95°C, 1 minute at 61°C, and 30 seconds at 72°C followed by 1 cycle of 10 minutes at 72°C. The PCR product was analyzed by size fractionation through a 1% agarose gel. Amplification of MTag gene results in a 480-bp fragment. All mice are congenic on the C57/BL6 background at $n \geq 10$. All mice were bred and maintained in specific pathogen-free conditions in the Mayo Clinic Scottsdale Natalie Schafer Transgenic Animal Facility. All experimental procedures were conducted according to Institutional Animal Care and Use Committee guidelines.

Celecoxib Treatment

Celecoxib was purchased from Pharmacia Pharmaceuticals (Skokie, IL) as 100-mg capsules. Drug was prepared for p.o. administration according to the manufacturer's recommendation.

Briefly, the drug was dissolved in DMSO, rotated at low speed in a 37°C hot room for 12 hours, and centrifuged at 1,800 rpm for 10 minutes, and the supernatant was collected and stored at 4°C as stock solution of 20 mg/mL. Ten-week-old female MTag mice were gavaged p.o. with 20-gauge barrel tip feeding needles (Fine Science Tools, Foster City, CA) at 5, 10, or 20 mg/kg body weight daily (5 days on with 2 days off) for 4 weeks. Control mice were gavaged with DMSO. Six mice per treatment group were used. Following 4 weeks of treatment, mice were sacrificed and mammary tumors dissected and divided into three parts: (*a*) to generate single cell suspension for flow cytometry, (*b*) to prepare tumor lysate for Western blot analysis and ELISA, and (*c*) to fix in formalin and embedded in paraffin blocks for immunohistochemical analysis. Serum was collected for ELISA. A dose range of 5 to 20 mg/kg body weight was used in our spontaneous mouse model based on previous reports in the literature (24, 34). These doses correspond to physiologic dose of celecoxib and are clinically relevant because the doses of COX-2 inhibitors recommended to patients are in the range of 5 to 20 mg/kg body weight (29).

Tumor Burden

From 10 weeks of age until sacrifice, control and celecoxib-treated mice were palpated weekly for presence of mammary tumors. Palpable tumors were measured by calipers and tumor weight was calculated according to the following formula: $g = L$ (cm) $\times$ W (cm^2) / 2 (39).

Analysis of Apoptosis by Flow Cytometry

Part of the tumor tissue was dissociated to generate single cell suspension by incubating in 5 mmol/L EDTA solution for 1 hour at 37°C. Apoptosis was determined by staining single cells (1×10^6) with Annexin V and propidium iodide using the BD PharMingen (San Diego, CA) apoptosis kit following the manufacturer's protocol. Cell staining was determined by flow cytometry using the CellQuest program. Percentage apoptotic cells were determined by CellQuest statistical analysis program as the cumulative percentage cells that were stained positive for both propidium iodide and Annexin V (upper right quadrant) and cells that were stained for Annexin V only (lower right quadrant).

Analysis of Apoptosis, Proliferation, and Blood Vessels by Immunohistochemistry

Part of the tumor was formalin fixed [10% neutral-buffered formalin (pH 6.8-7.2), Fisher Scientific, Pittsburgh, PA] and paraffin embedded and 5-μm sections were prepared by the Mayo Clinic Scottsdale Histology Core Facility. Immunohistochemistry was done using the ApopTag Peroxidase *In situ* Apoptosis Detection kit (Serologicals Corp., Norcross, GA). 3,3′-Diaminobenzidine was used as the chromogen and hematoxylin was used as counterstain. TUNEL-positive cells were examined under light microscopy and representative images taken at 200×. For PCNA staining, paraffin-embedded and 5-μm sections were subjected to antigen retrieval using the DAKO Target Retrieval (Carpinteria, CA) at 95°C for 40 minutes. Primary antibody (PCNA antibody, BD Biosciences,

San Jose, CA) was used at 5 μg/mL at 4°C overnight and DAKO anti-mouse secondary conjugated to horseradish peroxidase was used at 1:200 for 2 hours at room temperature. 3,3′-Diaminobenzidine was used as the chromogen and hematoxylin was used as counterstain. Histologic evaluation of vascularity was determined by Masson's trichrome staining (61). This method stains fibrous tissue and stroma green. Blood vessels containing RBC stain bright red.

Assay for Caspase-3 and Caspase-7

Primary MTag tumor cells derived from 17-week-old MTag mice were treated with increasing concentrations (20-60 μmol/L) of celecoxib or DMSO (vehicle) in medium supplemented with 5% FCS for 48 hours. To evaluate if celecoxib treatment can induce activation of caspase-3 and caspase-7, we detected levels of active forms of caspase-3 and caspase-7 in freshly prepared cell lysates from treated and untreated MTag tumor cells using the EnzChek Caspase-3/7 Assay Kit (Molecular Probes, Eugene, OR) following the manufacturer's protocol. In principle, active caspase-3 or caspase-7 will cleave a fluorogenic substrate releasing the fluorochrome, and the fluorescence was detected and quantified by spectrofluorometry using UV excitation of 380 nm and detected at an emission wavelength range of 430 to 460 nm. Fluorescence emission is an indication of caspase-3 and caspase-7 activity. Thus, apoptotic cell lysates containing active caspase-3 and caspase-7 yield considerable emission as compared with nonapoptotic lysates that do not contain the active forms of the enzymes.

ELISA for PGE$_2$ and VEGF

PGE$_2$ and VEGF enzyme immunoassay kits (Cayman Chemical Co., Ann Arbor, MI for PGE$_2$ and Oncogene Research Products, La Jolla, CA for VEGF) were used to assay the levels of PGE$_2$ and VEGF in tumor lysates and serum derived from treated and control mice. All tumor lysates were made in tissue lysis buffer containing 20 mmol/L HEPES, 0.15 mol/L NaCl, and 1% Triton X-100 supplemented with 80 μL/mL phosphatase inhibitor cocktail II (Sigma P-5726, St. Louis, MO) and 10 μL/mL complete protease inhibitor cocktail (Boehringer Mannheim GmbH, Indianapolis, IN). The PGE$_2$ and VEGF assays were done according to the manufacturer's recommendation. Lysates were diluted appropriately to ensure that readings were within the limits of accurate detection. Results are expressed as picogram of PGE$_2$ or VEGF per milliliter of serum or per microgram protein of tumor lysate for individual mice.

Western Blot Analysis for COX-2, Phospho-Akt, Bax, and Bcl-2

Tumor lysates from treated and untreated mice prepared as stated previously were resolved by SDS-PAGE on 10% to 15% resolving gels. Tumor lysate (100 μg) was loaded per lane. Gels were blotted and probed for COX-2 (p70, 1:200, Santa Cruz Biotechnology, Santa Cruz, CA), phospho-Akt and Akt protein (p60, 1:1,000, Cell Signaling, Beverly, MA), Bax-horseradish peroxidase conjugated (p23, 1:200, Santa Cruz Biotechnology), and Bcl-2 (p26, 1:1,000, Trevigen, Gaithersburg, MD). Mammary gland tumor lysates from 20- to 22-week-old MTag

mouse are used as positive control for COX-2. Jurkat T lymphoma cell lysate was used as positive control for the other proteins. Individual animal protein expression data are shown.

Statistical Analysis

All data are expressed as means ± SD. Statistically significant difference between experimental groups was assessed by one-way ANOVA with Dunnett adjustment.

References

1. Ellis MJ, Hayes DF, Lippman ME. Treatment of metastatic breast cancer. Diseases of the breast. In: Harris JR, Lippman ME, Morrow M, Osborne CK, editors. Philadelphia (PA): Lippincott Williams & Wilkins; 2000. p. 749 – 99.

2. Kujubu DA, Fletcher BS, Varnum BC, Lim RW, Herschman HR. TIS10, a phorbol ester tumor promoter-inducible mRNA from Swiss 3T3 cells, encodes a novel prostaglandin synthase/cyclooxygenase homologue. J Biol Chem 1991; 266:12866 – 72.

3. Kutchera W, Jones DA, Matsunami N, et al. Prostaglandin H synthase 2 is expressed abnormally in human colon cancer: evidence for a transcriptional effect. Proc Natl Acad Sci U S A 1996;93:4816 – 20.

4. Smith WL, Garavito RM, DeWitt DL. Prostaglandin endoperoxide H synthases (cyclooxygenases)-1 and -2. J Biol Chem 1996;271:33157 – 60.

5. Smith WL, DeWitt DL, Garavito RM. Cyclooxygenases: structural, cellular, and molecular biology. Annu Rev Biochem 2000;69:145 – 82.

6. Oshima M, Dinchuk JE, Kargman SL, et al. Suppression of intestinal polyposis in ApcΔ716 knockout mice by inhibition of cyclooxygenase 2 (COX-2). Cell 1996;87:803 – 9.

7. Subbaramaiah K, Zakim D, Weksler BB, Dannenberg AJ. Inhibition of cyclooxygenase: a novel approach to cancer prevention. Proc Soc Exp Biol Med 1997;216:201 – 10.

8. Taketo MM. Cyclooxygenase-2 inhibitors in tumorigenesis (Part II). J Natl Cancer Inst 1998;90:1609 – 20.

9. Eberhart CE, Coffey RJ, Radhika A, Giardiello FM, Ferrenbach S, DuBois RN. Up-regulation of cyclooxygenase 2 gene expression in human colorectal adenomas and adenocarcinomas. Gastroenterology 1994;107:1183 – 8.

10. Soslow RA, Dannenberg AJ, Rush D, et al. COX-2 is expressed in human pulmonary, colonic, and mammary tumors. Cancer 2000;89:2637 – 45.

11. Half E, Tang XM, Gwyn K, Sahin A, Wathen K, Sinicrope FA. Cyclooxygenase-2 expression in human breast cancers and adjacent ductal carcinoma *in situ*. Cancer Res 2002;62:1676 – 81.

12. Li M, Lotan R, Levin B, Tahara E, Lippman SM, Xu XC. Aspirin induction of apoptosis in esophageal cancer: a potential for chemoprevention. Cancer Epidemiol Biomarkers Prev 2000;9:545 – 9.

13. Zimmermann KC, Sarbia M, Weber AA, Borchard F, Gabbert HE, Schror K. Cyclooxygenase-2 expression in human esophageal carcinoma. Cancer Res 1999; 59:198 – 204.

14. Hosomi Y, Yokose T, Hirose Y, et al. Increased cyclooxygenase 2 (COX-2) expression occurs frequently in precursor lesions of human adenocarcinoma of the lung. Lung Cancer 2000;30:73 – 81.

15. Hida T, Yatabe Y, Achiwa H, et al. Increased expression of cyclooxygenase 2 occurs frequently in human lung cancers, specifically in adenocarcinomas. Cancer Res 1998;58:3761 – 4.

16. Uotila P, Valve E, Martikainen P, Nevalainen M, Nurmi M, Harkonen P. Increased expression of cyclooxygenase-2 and nitric oxide synthase-2 in human prostate cancer. Urol Res 2001;29:23 – 8.

17. Yoshimura R, Sano H, Masuda C, et al. Expression of cyclooxygenase-2 in prostate carcinoma. Cancer 2000;89:589 – 96.

18. Mohammed SI, Knapp DW, Bostwick DG, et al. Expression of cyclo-oxygenase-2 (COX-2) in human invasive transitional cell carcinoma (TCC) of the urinary bladder. Cancer Res 1999;59:5647 – 50.

19. Ristimaki A, Nieminen O, Saukkonen K, Hotakainen K, Nordling S, Haglund C. Expression of cyclooxygenase-2 in human transitional cell carcinoma of the urinary bladder. Am J Pathol 2001;158:849 – 53.

20. Tang Q, Gonzales M, Inoue H, Bowden GT. Roles of Akt and glycogen synthase kinase 3β in the ultraviolet B induction of cyclooxygenase-2 transcription in human keratinocytes. Cancer Res 2001;61:4329 – 32.

21. Neufang G, Furstenberger G, Heidt M, Marks F, Muller-Decker K. Abnormal differentiation of epidermis in transgenic mice constitutively expressing cyclooxygenase-2 in skin. Proc Natl Acad Sci U S A 2001;98:7629 – 34.

22. Tucker ON, Dannenberg AJ, Yang EK, et al. Cyclooxygenase-2 expression is up-regulated in human pancreatic cancer. Cancer Res 1999;59:987 – 90.

23. Molina MA, Sitja-Arnau M, Lemoine MG, Frazier ML, Sinicrope FA. Increased cyclooxygenase-2 expression in human pancreatic carcinomas and cell lines: growth inhibition by nonsteroidal anti-inflammatory drugs. Cancer Res 1999;59:4356 – 62.

24. Kundu N, Fulton AM. Selective cyclooxygenase (COX)-1 or COX-2 inhibitors control metastatic disease in a murine model of breast cancer. Cancer Res 2002;62:2343 – 6.

25. Gupta RA, Dubois RN. Colorectal cancer prevention and treatment by inhibition of cyclooxygenase-2. Nat Rev Cancer 2001;1:11 – 21.

26. Jacoby RF, Seibert K, Cole CE, Kelloff G, Lubet RA. The cyclooxygenase-2 inhibitor celecoxib is a potent preventive and therapeutic agent in the min mouse model of adenomatous polyposis. Cancer Res 2000;60:5040 – 4.

27. Reddy BS, Hirose Y, Lubet R, et al. Chemoprevention of colon cancer by specific cyclooxygenase-2 inhibitor, celecoxib, administered during different stages of carcinogenesis. Cancer Res 2000;60:293 – 7.

28. Schreinemachers DM, Everson RB. Aspirin use and lung, colon, and breast cancer incidence in a prospective study. Epidemiology 1994;5:138 – 46.

29. Steinbach G, Lynch PM, Phillips RK, et al. The effect of celecoxib, a cyclooxygenase-2 inhibitor, in familial adenomatous polyposis. N Engl J Med 2000;342:1946 – 52.

30. Williams CS, Watson AJ, Sheng H, Helou R, Shao J, DuBois RN. Celecoxib prevents tumor growth *in vivo* without toxicity to normal gut: lack of correlation between *in vitro* and *in vivo* models. Cancer Res 2000;60:6045 – 51.

31. Nakatsugi S, Ohta T, Kawamori T, et al. Chemoprevention by nimesulide, a selective cyclooxygenase-2 inhibitor, of 2-amino-1-methyl-6-phenylimidazo[4, 5-b]pyridine (PhIP)-induced mammary gland carcinogenesis in rats. Jpn J Cancer Res 2000;91:886 – 92.

32. Alshafie GA, Abou-Issa HM, Seibert K, Harris RE. Chemotherapeutic evaluation of celecoxib, a cyclooxygenase-2 inhibitor, in a rat mammary tumor model. Oncol Rep 2000;7:1377 – 81.

33. Rozic JG, Chakraborty C, Lala PK. Cyclooxygenase inhibitors retard murine mammary tumor progression by reducing tumor cell migration, invasiveness and angiogenesis. Int J Cancer 2001;93:497 – 506.

34. Blumenthal RD, Waskewich C, Goldenberg DM, Lew W, Flefleh C, Burton J. Chronotherapy and chronotoxicity of the cyclooxygenase-2 inhibitor, celecoxib, in athymic mice bearing human breast cancer xenografts. Clin Cancer Res 2001;7:3178 – 85.

35. Harris RE, Chlebowski RT, Jackson RD, et al. Breast cancer and nonsteroidal anti-inflammatory drugs: prospective results from the Women's Health Initiative. Cancer Res 2003;63:6096 – 101.

36. Guy CT, Cardiff RD, Muller WJ. Induction of mammary tumors by expression of polyomavirus middle T oncogene: a transgenic mouse model for metastatic disease. Mol Cell Biol 1992;12:954 – 61.

37. Cardiff RD, Muller WJ. Transgenic mouse models of mammary tumorigenesis. Cancer Surv 1993;16:97 – 113.

38. Maglione JE, Moghanaki D, Young LJ, et al. Transgenic polyoma middle-T mice model premalignant mammary disease. Cancer Res 2001;61:8298 – 305.

39. Mukherjee P, Madsen CS, Ginardi AR, et al. Mucin 1-specific immunotherapy in a mouse model of spontaneous breast cancer. J Immunother 2003;26: 47 – 62.

40. Paulson SK, Kaprak TA, Gresk CJ, et al. Plasma protein binding of celecoxib in mice, rat, rabbit, dog and human. Biopharm Drug Dispos 1999;20: 293 – 9.

41. Niederberger E, Tegeder I, Vetter G, et al. Celecoxib loses its anti-inflammatory efficacy at high doses through activation of NF-κB. FASEB J 2001;15:1622 – 4.

42. Basu GD, LaGioia M, Tinder TL, et al. The COX-2 selective inhibitor, celecoxib mediates growth inhibition in breast cancer cell lines via diverse pathways. Cancer Epidemiol Biomarkers Prev 2003;12:1298S.

43. Gavrieli Y, Sherman Y, Ben-Sasson SA. Identification of programmed cell death *in situ* via specific labeling of nuclear DNA fragmentation. J Cell Biol 1992;119:493–501.

44. Cao Y, Prescott SM. Many actions of cyclooxygenase-2 in cellular dynamics and in cancer. J Cell Physiol 2002;190:279–86.

45. Scheid MP, Woodgett JR. Unravelling the activation mechanisms of protein kinase B/Akt. FEBS Lett 2003;546:108–12.

46. Datta SR, Dudek H, Tao X, et al. Akt phosphorylation of BAD couples survival signals to the cell-intrinsic death machinery. Cell 1997;91:231–41.

47. del Peso L, Gonzalez-Garcia M, Page C, Herrera R, Nunez G. Interleukin-3-induced phosphorylation of BAD through the protein kinase Akt. Science 1997;278:687–9.

48. Cardone MH, Roy N, Stennicke HR, et al. Regulation of cell death protease caspase-9 by phosphorylation. Science 1998;282:1318–21.

49. Lai GH, Zhang Z, Sirica AE. Celecoxib acts in a cyclooxygenase-2-independent manner and in synergy with emodin to suppress rat cholangiocarcinoma growth *in vitro* through a mechanism involving enhanced Akt inactivation and increased activation of caspases-9 and -3. Mol Cancer Ther 2003;2:265–71.

50. Hsu AL, Ching TT, Wang DS, Song X, Rangnekar VM, Chen CS. The cyclooxygenase-2 inhibitor celecoxib induces apoptosis by blocking Akt activation in human prostate cancer cells independently of Bcl-2. J Biol Chem 2000;275:11397–403.

51. Chang SH, Liu CH, Conway R, et al. Role of prostaglandin E_2-dependent angiogenic switch in cyclooxygenase 2-induced breast cancer progression. Proc Natl Acad Sci U S A 2004;101:591–6.

52. Mukherjee P, Tinder TL, Basu GD, Pathangey LB, Chen L, Gendler SJ. Therapeutic efficacy of MUC1-specific cytotoxic T lymphocytes and CD137 co-stimulation in a spontaneous breast cancer model. Breast Dis. In press 2004.

53. Pockaj B, Basu GD, Pathangey LB, et al. Reduced T cell and dendritic cell function is related to COX-2 over-expression and PGE_2 secretion in patients with breast cancer. Ann Surg Oncol 2003;11:328–39.

54. Wang D, DuBois RN. Cyclooxygenase 2-derived prostaglandin E_2 regulates the angiogenic switch. Proc Natl Acad Sci U S A 2004;101:415–6.

55. Cantley LC. The phosphoinositide 3-kinase pathway. Science 2002;296:1655–7.

56. Soengas MS, Lowe SW. Apoptosis and melanoma chemoresistance. Oncogene 2003;22:3138–51.

57. Sheng H, Shao J, Morrow JD, Beauchamp RD, DuBois RN. Modulation of apoptosis and Bcl-2 expression by prostaglandin E_2 in human colon cancer cells. Cancer Res 1998;58:362–6.

58. Ben-Av P, Crofford LJ, Wilder RL, Hla T. Induction of vascular endothelial growth factor expression in synovial fibroblasts by prostaglandin E and interleukin-1: a potential mechanism for inflammatory angiogenesis. FEBS Lett 1995;372:83–7.

59. Seno H, Oshima M, Ishikawa TO, et al. Cyclooxygenase 2- and prostaglandin E(2) receptor EP(2)-dependent angiogenesis in Apc(Δ716) mouse intestinal polyps. Cancer Res 2002;62:506–11.

60. Breyer RM, Bagdassarian CK, Myers SA, Breyer MD. Prostanoid receptors: subtypes and signaling. Annu Rev Pharmacol Toxicol 2001;41:661–90.

61. Jadeski LC, Lala PK. Nitric oxide synthase inhibition by *N*(G)-nitro-L-arginine methyl ester inhibits tumor-induced angiogenesis in mammary tumors. Am J Pathol 1999;155:1381–90.

Cyclooxygenase-2 Inhibitor Induces Apoptosis in Breast Cancer Cells in an *In vivo* Model of Spontaneous Metastatic Breast Cancer [1] [1]Susan G. Komen Breast Cancer Foundation.
Note: G.D. Basu and L.B. Pathangey contributed equally to this work.

Gargi D. Basu, Latha B. Pathangey, Teresa L. Tinder, et al.

Updated version	Access the most recent version of this article at: http://mcr.aacrjournals.org/content/2/11/632

Cited articles	This article cites 58 articles, 30 of which you can access for free at: http://mcr.aacrjournals.org/content/2/11/632.full#ref-list-1
Citing articles	This article has been cited by 13 HighWire-hosted articles. Access the articles at: http://mcr.aacrjournals.org/content/2/11/632.full#related-urls

E-mail alerts	Sign up to receive free email-alerts related to this article or journal.
Reprints and Subscriptions	To order reprints of this article or to subscribe to the journal, contact the AACR Publications Department at pubs@aacr.org.
Permissions	To request permission to re-use all or part of this article, use this link http://mcr.aacrjournals.org/content/2/11/632. Click on "Request Permissions" which will take you to the Copyright Clearance Center's (CCC) Rightslink site.